PHYSICAL ELECTRONICS

Original article
DOI: https://doi.org/10.18721/JPM.19208

THE INFLUENCE OF AR^+ AND CD^+ ION IMPLANTATION ON THE COMPOSITION AND ELECTRONIC STRUCTURE OF MONOCRYSTALLINE ZINC TELLURIDE

J. B. Khujaniyozov[1]✉, B. E. Umirzakov[1], D. A. Tashmukhamedova[1], V. V. Loboda[2], A. A. Abduvayitov[1]

[1] Tashkent State Technical University Named after Islam Karimov,

Tashkent, Republic of Uzbekistan;

[2] Peter the Great St. Petersburg Polytechnic University, St. Petersburg, Russia

✉ KhujaniyozovJB@mail.ru

Abstract. The effect of Ar^+ and Cd^+ ion implantation and subsequent thermal annealing has been studied on a single-crystal ZnTe (111) using a whole range of spectroscopy methods: ultraviolet photoelectron one (UPS), light absorption one, and Auger electron one (AES). The results showed that bombardment of the surface with Ar^+ and Cd^+ ions with an energy of E_0 = 1 keV until a saturation dose of of D_{sat} = (6–8)·10^{16}cm^{-2} was reached resulted in the destruction of the crystal structure of the ion-implanted layers and, as a consequence, in surface metallization. In particular, after implantation with Cd^+ ions and subsequent annealing at T = 850 K, the formation of a homogeneous continuous $Zn_{0.5}Cd_{0.5}Te$ film 30–35 Å thick was observed, which indicated the redistribution of components and the formation of a new phase state on the ZnTe surface. The results of the study of $Zn_{0.5}Cd_{0.5}Te$ thin films demonstrate the presence of two clearly defined maxima in the valence electron spectra corresponding to binding energies of −1.4 eV and −5.2 eV.

Keywords: heterostructure, photoelectron spectroscopy, implantation, molecular beam epitaxy, saturation dose, thin film, zinc telluride

Citation: Khujaniyozov J. B., Umirzakov B. E., Tashmukhamedova D. A., Loboda V. V., Abduvayitov A. A., The influence of $Ar^+$and Cd^+ ion implantation on the composition and electronic structure of monocrystalline zinc telluride, St. Petersburg State Polytechnical University Journal. Physics and. 19 (2) (2026) 84–97. DOI: https://doi.org/10.18721/JPM.19208

This is an open access article under the CC BY-NC 4.0 license (https://creativecommons.org/ Mathematics licenses/by-nc/4.0/)

© Khujaniyozov J. B., Umirzakov B. Y., Tashmukhamedova D. A., Loboda V. V., Abduvayitov A. A., 2026. Published by Peter the Great St. Petersburg Polytechnic University.

Научная статья
УДК 538.971:621.315.592
DOI: https://doi.org/10.18721/JPM.19208

ВЛИЯНИЕ ИМПЛАНТАЦИИ ИОНОВ AR^+ И CD^+ НА СОСТАВ И ЭЛЕКТРОННУЮ СТРУКТУРУ МОНОКРИСТАЛЛИЧЕСКОГО ТЕЛЛУРИДА ЦИНКА

Ж. Б. Хужаниёзов[1]✉, *Б. Е. Умирзаков*[1], *Д. А. Ташмухамедова*[1], *В. В. Лобода*[2], *А. А. Абдувайитов*[1]

[1] Ташкентский государственный технический университет им. Ислама Каримова, г. Ташкент, Узбекистан;

[2] Санкт-Петербургский политехнический университет Петра Великого, Санкт-Петербург, Россия

✉ KhujaniyozovJB@mail.ru

Аннотация. Влияние ионной имплантации Ar^+ и Cd^+, а также последующего термического отжига было изучено на монокристаллическом образце ZnTe(111) с применением комплекса методов спектроскопии: ультрафиолетовой фотоэлектронной, поглощения света в УФ-. ИК-, видимой областях и Оже-электронной. Результаты исследований показали, что бомбардировка поверхности ионами Ar^+ и Cd^+ с энергией E_0 = 1 кэВ до достижения дозы насыщения D_{sat} = (6−8)·10^{16} $см^{-2}$ приводит к разрушению кристаллической структуры ионно-имплантированных слоев и, как следствие, к металлизации поверхности. В частности, после имплантации ионами Cd^+ и последующего отжига при температуре T = 850 K наблюдается формирование гомогенной сплошной пленки $Zn_{0,5}Cd_{0,5}Te$ толщиной 30 − 35 Å, что свидетельствует о перераспределении компонентов и образовании нового фазового состояния на поверхности ZnTe. Результаты исследования тонких пленок $Zn_{0,5}Cd_{0,5}Te$ демонстрируют наличие двух отчетливо выраженных максимумов в спектрах валентных электронов, соответствующих энергиям связи −1,4 эВ и −5,2 эВ.

Ключевые слова: гетероструктура, фотоэлектронная спектроскопия, имплантация, молекулярно-лучевая эпитаксия, доза насыщения, тонкая пленка, теллурид цинка

Ссылка для цитирования: Хужаниёзов Ж. Б., Умирзаков Б. Е., Ташмухамедова Д. А., Лобода В. В., Абдувайитов А. А. Влияние имплантации ионов Ar^+ и Cd^+ на состав и электронную структуру монокристаллического теллурида цинка // Научно-технические ведомости СПбГПУ. Физико-математические науки. 2026. Т. 19. № 2. С. 84−97. DOI: https://doi.org/10.18721/JPM.19208

Статья открытого доступа, распространяемая по лицензии CC BY-NC 4.0 (https://creativecommons.org/licenses/by-nc/4.0/)

Introduction

$A^{II}B^{VI}$ semiconductors such as cadmium and zinc tellurides (CdTe, ZnTe) have long served as model objects for fundamental research; however, their practical application remained relatively limited, being mainly confined to X-ray detectors and luminophores. Nevertheless, these compounds are characterized by high structural perfection and possess unique optical properties.

In recent years, $A^{II}B^{VI}$ compounds have attracted increasing attention as promising materials for efficient conversion of solar energy into electricity, owing to their high quantum yield in the green spectral region [1−5].

One of the factors hindering the widespread use of heterostructures based on CdTe and ZnTe is the significant mismatch in their lattice parameters. The resulting mechanical stresses at interfaces can lead to degradation and failure of the structures. The lattice mismatch also introduces

© Хужаниёзов Ж. Б., Умирзаков Б. Е., Ташмухамедова Д. А., Лобода В. В., Абдувайитов А. А., 2026. Издатель: Санкт-Петербургский политехнический университет Петра Великого.

uncertainties in the accurate determination of the band offset, reflected in a substantial scatter (up to ±10% of the average bandgap) in the published data on the valence band offset of CdTe/ZnTe heterostructures [6–9].

Studies on heterostructures based on binary semiconductors [10–18], in particular, the CdTe/ZnTe system with identical nominal thickness of the narrow-gap layer, demonstrate a significant discrepancy in the energy position and shape of the emission band. This points to a pronounced dependence of the actual structure of the thin layer on the specific growth conditions. For the CdTe/ZnTe system, this aspect is of particular importance in the context of developing CdTe quantum dots doped with a precisely controlled amount of Mn^{2+} magnetic ions [19].

Stresses arising during growth and their subsequent relaxation play a key role for heteroepitaxial structures. These processes have a decisive influence on the crystalline perfection of the structure, which, in turn, directly affects the electronic properties of the material and, consequently, the parameters of fabricated infrared detectors [20–28]. A wide range of optical [24] and X-ray diffraction [25, 26] methods are used for high-precision measurements of residual strains occurring in the bulk of the material, providing valuable information on the mechanical state of the structure.

Ref. [28] reports on an experimental study of weak strains in the near-surface regions of amorphous chromium (Cr) and mercury-cadmium telluride (HgCdTe) layers using an innovative null method. The study yielded quantitative data demonstrating the dependence of the second-harmonic amplitude on the magnitude of applied stresses. In addition, precision measurements of residual stresses in the surface layer of a multilayered HgCdTe/CdTe/ZnTe/GaAs structure grown by molecular beam epitaxy were performed, which made it possible to establish the parameters of the structure's stressed state.

The method of low-energy ion implantation has proven to be an effective tool for targeted modification of the composition, structure and properties of various materials [29–37], opening new prospects in materials science and surface engineering.

The present work reports on the surface modification of monocrystalline zinc telluride (ZnTe) films by implantation of argon Ar^+ and cadmium Cd^+ ions combined with thermal treatment.

The goal of this study is a detailed investigation of the mechanisms leading to changes in the elemental composition and electronic structure of zinc telluride films as a result of a complex treatment.

Experimental procedure

The film samples were studied using an ultra-high-vacuum system (Fig. 1) consisting of two functionally separated chambers.

Annealing, thermal oxidation and ion bombardment procedures were carried out in the first chamber; these procedures prepared the materials for further analysis.



Fig. 1. Experimental setup

The second chamber was used for detailed analysis of the composition, density of states of valence electrons, band structure, as well as emission and optical characteristics of the samples.

Polished and chemically etched monocrystalline ZnTe(111) samples and epitaxial *n*-type ZnTe/Si(111) films grown by magnetron sputtering were used for the study.

The experiments were performed under high vacuum (pressure down to 10^{-7} Pa) using a combination of spectroscopic methods: Auger electron spectroscopy (AES), ultraviolet photoelectron spectroscopy (UPS), optical absorption spectroscopy in the UV, IR and visible ranges, and elastic peak electron spectroscopy (EPES).

Depth profiles of atomic distributions were determined by AES combined with precision layer-by-layer sputtering of the surface with Ar^+ ions at an energy E_0 ranging from 2 to 3 keV. Prior to ion implantation,

the ZnTe samples were degassed by heating to $T = 900$ K for three hours. This process was combined with Ar^+ ion sputtering at a pressure of 10^{-7} Pa to remove surface contaminants.

After cleaning, the Auger peaks corresponding to carbon (C), sulfur (S) and oxygen (O) completely disappeared, indicating a high degree of surface purity. The concentrations of zinc (Zn) and tellurium (Te) atoms stabilized within the range of about 49–50 at.%, which indicated the restoration of the stoichiometric composition.

Cd^+ ions were implanted at an energy $E_0 = 3–1$ keV with a dose $D = 8 \cdot 10^{16}$ cm^{-2}; this value corresponded to the saturation dose, at which further increase in dose did not lead to significant changes in the material properties. The Cd^+ ions were generated by electron bombardment, which provided high precision control of the ion beam parameters.

Experimental results and discussion

Fig. 2 shows the change in the surface concentration of zinc in ZnTe under bombardment with Ar^+ ions at an energy $E_0 = 1$ keV at room temperature.

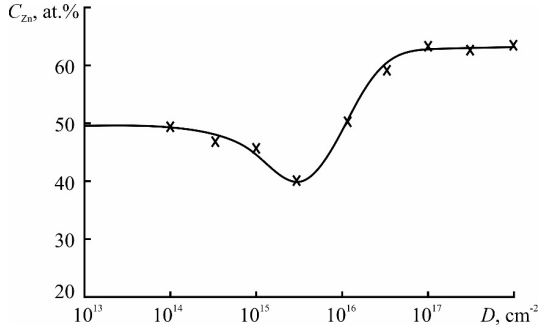


Fig. 2. Dependence of the surface zinc concentration in ZnTe/Si(111) film on the irradiation dose after bombardment with 1 keV Ar^+ ions at room temperature

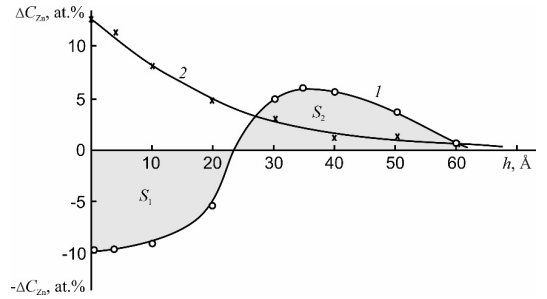


Fig. 3. Dependences of deviation ДΔC_{Zn} on depth of ZnTe/Si(111) film bombarded with 1 keV Ar^+ ions at doses D (cm^{-2}): $5 \cdot 10^{15}$ (curve *1*) and $6 \cdot 10^{16}$ (curve *2*)

It can be seen that the surface Zn concentration C_{Zn} remains practically unchanged up to a dose $D = 10 \cdot 2^{14}$ cm^{-2}, indicating the stability of the material surface at the initial stage of ion exposure. Then, a decrease in the Zn concentration by 7–8 at.% is observed in the dose range from $2 \cdot 10^{14}$ to $5 \cdot 10^{15}$ cm^{-2}. A further increase in the ion dose leads to an increase in C_{Zn}, reaching 65–66 at.% at $D = (6–4) \cdot 10^{16}$ cm^{-2}. After that, further irradiation causes stabilization of the zinc concentration, which then undergoes virtually no changes.

To comprehensively analyze the modification of the surface concentration of Zn and Te atoms during Ar^+ ion bombardment, the depth dependence of the deviation ΔC_{Zn} of Zn concentration from the stoichiometric composition was studied at two different irradiation doses: $5 \cdot 10^{15}$ and $6 \cdot 10^{16}$ cm^{-2} (Fig. 3).

It follows from the data in Fig. 3 that a decrease in the Zn concentration by 8–10 at.% is observed at a dose of $D = 5 \cdot 10^{15}$ cm^{-2} in the near-surface layers, remaining almost unchanged down to a depth $h = 5–6$ Å. An increase in ΔC_{Zn} to about 6 at.% is observed in the range $h = 10–40$ Å. With a further increase in depth, ΔC_{Zn} decreases monotonically, tending to zero at $h = 60–65$ Å, which indicates the restoration of the stoichiometric composition characteristic of ZnTe. The decrease in Zn concentration in the range $h = 0–20$ Å is presumably due to the diffusion of Zn atoms deeper into the target or (less likely) to the diffusion of Te atoms to the surface (taking into account the significant difference in the masses of Te and Zn atoms). It is evident that the areas S_1 and S_2 under curve *1* differ only slightly, which suggests that there is no appreciable evaporation of Zn (or Te) atoms. At higher bombardment doses ($D \geq 6 \cdot 10^{16}$ cm^{-2}, see curve *2* in Fig. 3), the value of ΔC_{Zn} in the near-surface layers increases to 10–12 at.%, then decreases monotonically with increasing h. At a depth of 50–60 Å, the value of ΔC_{Zn} is about 1–2 at.%, remaining practically unchanged at $h \geq 60$ Å.

In all probability, desorption of Te atoms from the surface layers occurs at high ion bombardment doses along with their diffusion to the surface, leading to metallization of the surface layers of the ZnTe film. In this case, the surface layers become completely disordered.

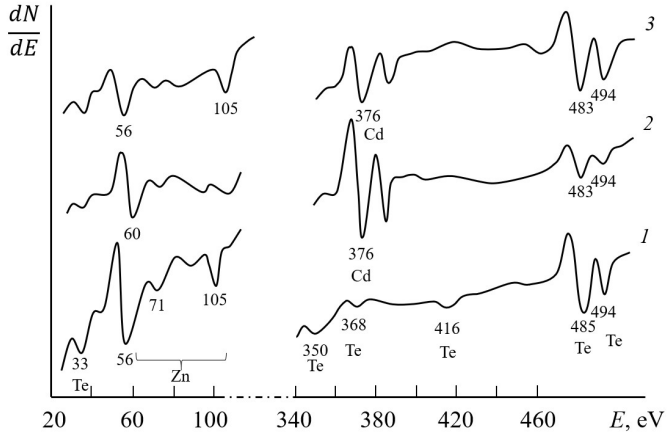


Fig. 4. Auger spectra of samples at different stages of the study:
as-grown ZnTe(111) sample (curve *1*); sample after implantation with Cd^+ (E_0 = 1 keV, $D_s = 8 \cdot 10^{16}$ cm^{-2}) (curve *2*); sample after ion implantation and annealing at T = 850 K for 40 min (curve *3*). The numbers correspond to the positions of the peaks (eV)

Fig. 4 shows the Auger spectra of ZnTe samples implanted with Cd^+ ions at an energy E_0 = 1 keV and a dose $D_s = 8 \cdot 10^{16}$ cm^{-2}, recorded before and after annealing at T = 850 K for 40 min. It is known that analysis of the shift and shape of low-energy peaks induced by the participation of valence electrons provides data on the formation of new compounds.

The atomic concentration C_x in the near-surface layers can be estimated from the intensities of the high-energy peaks using the following formula [38]:

$$C_x = \frac{I_x / S_x}{\sum_{i=1} \frac{I_i}{S_i}},$$

where I_i, I_x are the intensities of the Auger peaks, S_i, S_x are the Auger sensitivity factors.

The following Auger peaks were used to determine the atomic concentrations:

Zn: E = 994 eV; Te: E = 483 eV; Cd: E = 376 eV.

The characteristic Zn and Te peaks are clearly observed in the Auger spectrum of the unimplanted ZnTe film. Quantitative analysis of the spectra showed that the surface concentration of Zn was about 49 at.%, and that of Te about 51 at.%. Implantation of Cd^+ ions causes decomposition of the ZnTe compound with simultaneous incorporation of Cd atoms into the ZnTe lattice. Distinct Zn and Cd peaks are observed in the Auger spectrum after ion implantation, while the intensity of Te peaks decreases significantly, so that low-intensity peaks disappear completely, which indicates predominant desorption of Te atoms from the sample surface. The main low-energy peak (56 eV) characteristic of ZnTe shifts by 4 eV towards higher energies. This is because Cd^+ ion implantation induces decomposition of the original ZnTe sample and a sharp decrease in Te concentration; as a result, the peak energy approaches the value characteristic of pure Zn. Analysis of the high-energy peaks of the full Auger spectrum revealed that the surface concentrations of Cd, Zn and Te atoms were approximately 48, 40, and 12 at.%, respectively.

After annealing at 850 K for 40 min, the 60 eV peak shifts back towards lower energies. The concentrations of Cd and Zn atoms decrease to 23–25 at.%, while that of Te increases to 50–52 at.%, indicating the formation of a monocrystalline film with an approximate composition $Zn_{0.5}Cd_{0.5}Te$ (see curve *3* in Fig. 4).

The electronic structure of the surface layers, including the density of electronic states and band parameters, was studied by ultraviolet photoelectron spectroscopy (UPS) and optical absorption spectroscopy [39].

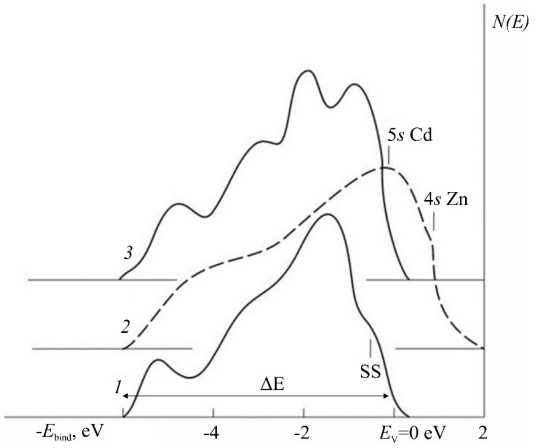


Fig. 5. UPS spectra recorded at different stages of the study: as-grown ZnTe(111) sample (curve *1*); sample after implantation with Cd^+ ions (E_0 = 1 keV, D_s = $8 \cdot 10^{16}$ cm^{-2}) (curve 2); sample after ion implantation and annealing at T = 850 K for 40 min (curve *3*); SS denotes surface states

Fig. 5 shows photoelectron spectra recorded at a photon energy $h\nu$ = 10.8 eV for a ZnTe sample implanted with Cd^+ ions at an energy E_0 = 1 keV and a dose $D = 8 \cdot 10^{16}$ cm^{-2}, before and after thermal annealing at T = 850 K.

Two well-defined peaks are clearly observed in the spectrum of pure ZnTe at binding energies of about −1.4 and −5.2 eV, as well as a characteristic feature at E_{SS} = −0.5 eV, presumably related to the existence of surface states. Detailed information on the possible mechanisms behind the formation of these peaks is given in Table 1.

Analysis of the data in Table 1 shows that the spectral peaks of pure ZnTe originate from the excitation of electrons from hybridized 4*s* Zn + 5*p* Te states and 5*s* Te states. Ion implantation leads to a shift of the leading edge of the spectrum towards higher energies, reaching about 1.8 eV. In addition, an increase in the spectral width (ΔE) is observed, the main peaks characteristic of ZnTe(111) disappear, and new peaks appear, which are likely associated with the formation of Zn, Cd inclusions and their compounds (see Table 1). In this case, the positions of the valence band top E_v and the Fermi level E_F coincide completely, indicating the metallic character of the ion-implanted layers. A characteristic spectral feature, accompanied by the appearance of four distinct peaks, is observed in the spectrum of the $Zn_{0.5}Cd_{0.5}Te$ film obtained after thermal annealing of the ion-implanted ZnTe at T = 850 K. A detailed interpretation of these peaks is also given in Table 1. Importantly, the position of the E_v level shifts towards lower energies by about 2 eV.

The bandgap width of the studied samples was estimated from the optical absorption (transmittance) spectra.

Table 1

Stages of UPS analysis of samples subjected to Cd^+ ion bombardment and annealing; interpretation of the results

Stage	Sample	UPS result	
		E_{bind}, eV	Peak formation mechanism
1. Initial	ZnTe (111)	–0.5	Surface state (SS)
		–1.4	4*s* Zn + 5*p* Te
		–5.2	5*s* Te
2. Implantation E_0 = 1 keV, $D_s = 8 \cdot 10^{16}$ cm^{-2}	ZnTe	+0.2	5*s* Cd
		+0.8	4*s* Zn
		–3.8	5*s* Te
3. Annealing at T = 850 K	$Zn_{0.5}Cd_{0.5}Te$/ZnTe	–0.3	Surface state (SS)
		–0.8	4*s* Zn + 5*p* Te
		–1.8	5*s* Cd + 5*p* Te
		–2.8	4*s* Zn + 5*p* Te
		–4.6	5*s* Te

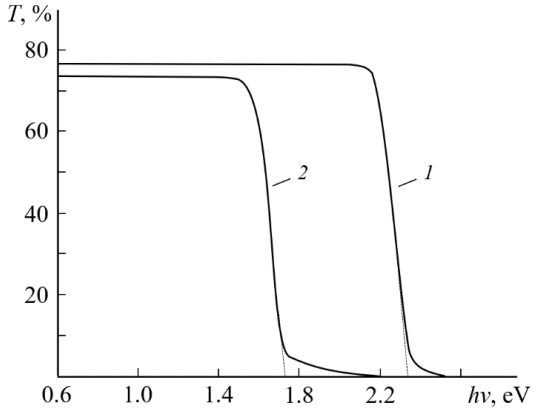


Fig. 6. Dependences of optical transmittance on photon energy for the as-grown ZnTe sample (curve *1*) and the final $Zn_{0.5}Cd_{0.5}Te$/ZnTe(111) film (curve *2*).
Film thickness was 30–35 Å, room temperature

Fig. 6 shows the dependences of the transmittance T_{ph} on the photon energy $h\nu$ for pure ZnTe(111) and for the $Zn_{0.5}Cd_{0.5}Te$/ZnTe(111) film obtained by post-implantation annealing at $T = 850$ K. Analysis of Fig. 6 shows that the transmittance of the pure ZnTe sample remains practically unchanged up to a photon energy of about 2.1 eV, indicating the absence of noticeable light absorption in this spectral region. A sharp drop in transmittance to zero is observed in the energy range $h\nu = 2.1$–2.3 eV, caused by intense light absorption. Extrapolation of this segment of the curve to the $h\nu$ axis allows approximately estimating the bandgap width E_g. Similarly, the E_g value for the $Zn_{0.5}Cd_{0.5}Te$ film was found to be approximately 1.75 eV. It should be noted that in the second case, the sharp decrease in T_{ph} begins already at about 1.7 eV, but complete absorption is reached only at about 2.2 eV. Apparently, ultra-thin films (less than 40 Å) exhibit some residual transparency even at $h\nu > E_g$, transmitting low-intensity light.

Table 2 presents the band and optical parameters derived from the photoelectron and optical absorption spectra for the initial and final samples (ZnTe and $Zn_{0.5}Cd_{0.5}Te$/ZnTe, respectively).

The energy of the valence band top E_v was determined as the difference between the photon energy and the width of the photoelectron spectrum:

$$E_v = h\nu - \Delta E.$$

The optical parameters of the samples were determined at a photon energy $h\nu = 1.2$ eV. Analyzing the data in Table 2, we find significant differences in the band and optical parameters of the $Zn_{0.5}Cd_{0.5}Te$ film and the ZnTe substrate. In particular, the bandgap width for the three-component film is about 1.75 eV, while for the substrate it is 2.35 eV. Subsequent studies revealed that the value of x in the $Zn_{1-x}Cd_x$ system reached 0.6 upon increasing the annealing temperature to 900 K, and grew to 0.8 at 950 K Upon a further increase in temperature in the range of 1000–1050 K, complete evaporation of cadmium atoms from the film occurred. Variation of the Cd^+ bombardment energy in the range from 1 to 10 keV will allow for controllable modifications in the thickness of the $Zn_{1-x}Cd_xTe$ film from 30–35 Å to 900–1000 Å, which opens up attractive prospects for precise tuning of material properties.

Table 2

Band and optical parameters of the films obtained from UPS and optical transmittance spectra

Experimental sample	Band energy parameters (eV)			Optical parameters at $h\nu = 1.2$ eV		
	E_v	E_g	X	R	T_{ph}	K
ZnTe	5.30	2.35	2.95	22	78	0
$Zn_{0.5}Cd_{0.5}Te$	5.35	1.75	3.6	26	74	

Notations: E_v is the energy of the valence band top, E_g is the bandgap width; χ is the electron affinity; R, T_{ph}, K are the reflectance, transmittance and absorptance, respectively; $h\nu$ is the photon energy.

Conclusion

For the first time, we comprehensively analyzed the effect of bombardment of the surface of zinc telluride (ZnTe) films with low-energy argon (Ar^+) and cadmium (Cd^+) ions on changes in the elemental composition and electronic structure of the near-surface layers.

It was found that irradiation with Ar^+ ions in the low-dose range ($D \leq 10 \cdot 5^{15}$ cm^{-2}) led to enrichment of the ZnTe surface with tellurium atoms, while a predominance of zinc atoms was observed with at higher doses ($D \geq 5 \cdot 10^{15}$ cm^{-2}); implantation of Cd^+ ions caused accumulation of Zn and Cd atoms on the ZnTe surface.

Thin films of the $Zn_{0.5}Cd_{0.5}Te$ solid solution with a uniform thickness in the range of 30–35 Å were formed by implanting Cd^+ ions into monocrystalline ZnTe followed by controlled annealing at 850 K.

Photoelectron spectroscopy and optical transmittance spectroscopy were used to obtain the distribution of the density of states of valence electrons, the energy band parameters and the optical characteristics of the grown $Zn_{0.5}Cd_{0.5}Te$ thin films. Two distinct maxima in the density of states were observed in the valence electron spectra of $Zn_{0.5}Cd_{0.5}Te$ at binding energies of −1.4 and −5.2 eV. These maxima correspond to specific features of the electron density distribution in the valence band of the material under study.

REFERENCES

1. **Iniewski K.,** CdTe and CdZnTe materials: Material properties and applications, Springer, Cham, Switzerland, 2024.

2. **Suthar D., Chuhadiya S., Sharma R., et al.,** An overview on the role of ZnTe as an efficient interface in CdTe thin film solar cells: A review, Mater. Adv. 3 (22) (2022) 8081–8107.

3. **Zhao Y., Jia Z., Lin Q.,** Optoelectronic properties and charge carrier dynamics of polycrystalline ZnTe thin films, J. Phys. Chem. Lett. 16 (24) (2025) 5979–5985.

4. **Yılmaz S., Başol B. M., Olğar M. A., et al.,** Comparative analysis of chloride-treated ZnTe films in photodetector devices, Mat. Sci. Semicond. Process. 198 (1 Nov) (2025) 109733.

5. **Zhang L., Liu C., Yang Q., et al.,** Growth and characterization of highly Nitrogen doped ZnTe films on GaAs (001) by molecular beam epitaxy, Mat. Sci. Semicond. Process. 29 (Jan) (2015) 351–356.

6. **Ergashov Y. S., Tashmukhamedova D. A., Djurabekova F. G., Umirzakov B. E.,** Effect of surface microroughness on the composition and electronic properties of CdTe/Mo(111) films, Bull. Russ. Acad. Sci., Phys. 80 (2) (2016) 138.

7. **Bagaev V. S., Zaytsev V. V., Kalinin V. V., et al.,** Excitonic luminescence of CdTe and $Cd_{0.87}Zn_{0.13}Te$ submonolayers in ZnTe films grown by molecular beam epitaxy, Solid State Commun. 88 (10) (1993) 777-780.

8. **Karczewski G., Maćkowski S., Kutrowski M., et al**., Photoluminescence study of CdTe/ZnTe self-assembled quantum dots, Appl. Phys. Lett. 74 (20) (1999) 3011–3013.

9. **Moger S. N., Mahesha M. G.,** Investigation on ZnTe/$Cd_xZn_{1-x}Te$ heterostructure for photodetector applications, Sens. Actuat. A-Phys. 315 (1 Nov) (2020) 112294.

10. **Hernández C. V.,** Introduction to Raman spectroscopy and its applications, Springer Cham, Switzerland, 2025.

11. **Kapitonov A. M., Woggon U., Kayser D., et al.,** Luminescence of epitaxial sub-monolayer CdSe nanostructures in ZnSe, J. Lumin. 112 (1–4) (2005) 177–180.

12. **Kim J. S., Kim H. M., Park H. L., Choi J. C.,** Growth and optical characterization of single quantum well structure of submonolayer ZnS/ZnTe, Solid State Commun. 137 (3) (2006) 115–119.

13. **Umirzakov B. E., Tashmukhamedova D. A., Boltaev E. U., Dzhurakhalov A. A., O**btaining of epitaxial films of metal silicides by ion implantation and molecular beam epitaxy, Mater. Sci. Eng. B. 101 (1–3) (2003) 124–127.

14. **Kryshtab T., Andraca J. A., Borkovska L. V., et al.,** Effect of CdTe monolayer insertion on CdZnTe/ZnTe quantum well characteristics, Microelectron. J. 39 (3–4) (2008) 418–422.

15. **Fan J., Ouyang L., Liu X., et al,** Growth and material properties of ZnTe on GaAs, InP, InAs and GaSb (001) substrates for electronic and optoelectronic device applications. J. Cryst. Growth. 323 (1) (2011) 127–131.

16. **Umirzakov B. E., Donaev S. B.,** On the creation of ordered nuclei by ion bombardment for obtaining nanoscale Si structures on the surface of CaF_2 films, J. Surf. Invest.: X-Ray, Synchrotron Neutron Tech. 11 (4) (2017) 746–748.

17. **Agekyan V., Chukeev M.**, **Karczewski G., et al.,** Exciton spectra and energy transfer in CdTe/ZnTe double quantum wells grown by atomic-layer epitaxy, Semiconductors. 53 (16) (2019) 2060–2063.

18. **Abduvayitov A. A., Boltaev Kh. Kh., Umirzakov B. E., et al.,** Analyzing the change in the composition of a CdTe surface upon implanting ions O^{2+} and subsequent annealing. Bull. Russ. Acad. Sci.: Phys. 88 (11) (2024) 1850–1854.

19. **Sawicki K., Malinowski F. K., Galkowski K., et al.,** *Single-color*, *in situ* photolithography marking of individual CdTe/ZnTe quantum dots containing a single Mn^{2+} ion, Appl. Phys. Lett. 106 (1) (2015) 012101.

20. **Samin A. J., Petrosky J. C.,** An analysis of point defects in ZnTe using density functional theory calculations, J. Alloys Compnd. 921 (15 Nov) (2022) 166017.

21. **Ryzhkov M. S., Kozlov D. A., Khudaiberdiev D. A., et al.,** Interference transport in a two-dimensional topological insulator in a CdHgTe quantum well, JETP Letters. 117 (1) (2023) 44–47.

22. **Shcherbakov I. P., Dunaev A. A., Eron'ko S. B., Chmel' A. E.,** Spectroscopic investigation of impurity and intrinsic distortions of the crystallite structure in ZnTe ceramics during mechanical treatment, Tech. Phys. Lett. 47 (2) (2021) 181–183.

23. **Tarasov A. S., Mikhailov N. N., Dvoretsky S. A., et al.,** Preparation of atomically clean and structurally ordered surfaces of epitaxial CdTe films for subsequent epitaxy, Semiconductors. 55 (1) (2021) S62–S66.

24. **Martinez A. M., Giudici P., Trigubo A. B., et al.,** Crystalline quality, composition homogeneity, tellurium precipitates/inclusions concentration, optical transmission, and energy band gap of Bridgman grown single-crystalline $Cd_{1-x}Zn_xTe$ ($0 \le x \le 0.1$), Materials. 14 (15) (2021) 4207.

25. **Dvoretsky S. A., Stupak M. F., Mikhailov N. N., et al.,** Study of the crystalline state of MBE (013)HgCdTe/CdTe/ZnTe/GaAs heterostructure layers by the second harmonic generation method, Semiconductors. 56 (8) (2022) 562–569.

26. **Stupak M. F., Mikhailov N. N., Dvoretskii S. A., et al.,** Possibilities of characterizing the crystal parameters of $Cd_xHg_{1-x}Te$ structures on GaAs substrates by the method of generation of the probe-radiation second harmonic in reflection geometry, Physics of the Solid State. 62 (2) (2020) 252–259.

27**. Ushakov V. V., Klevkov Yu. V.,** Microphotoluminescence of undoped single-crystal zinc telluride produced by nonequilibrium vapor-phase growth techniques, Semiconductors. 39 (9) (2005) 993–997.

28. **Stupak M. F., Dvoretsky S. A., Mikhailov N. N., et al.,** Measurement of local stresses in the surface layers of multilayer structures by the null method using phase matching, Tech. Phys. Lett. 50 (1) (2024) 32–35.

29. **Chemam R., Bouabellou A., Grob J. J., et al.,** ZnTe formed by ion implantation in a SiO_2 layer on silicon, Nucl. Instrum. Methods Phys. Res. B. 216 (Febr) (2004) 116–120.

30. **Umirzakov B. E., Tashmukhamedova D. A., Ruzibaeva M. K., et al.,** Investigation of change of the composition and structure of the CaF_2/Si films surface at the low-energy bombardment, Nucl. Instrum. Methods Phys. Res. B. 326 (1 May) (2014) 322–325.

31. **Isakhanov Z. A., Mukhtarov Z. E., Umirzakov B. E., Ruzibaeva M. K.,** Optimum ion implantation and annealing conditions for stimulating secondary negative ion emission, Tech. Phys. 56 (4) (2011) 546–549.

32. **Hassan A. M., Diab F., Kotp E. F., et al.,** Implantation of Cu onto ZnTe thin film using plasma focus device for optoelectronic applications, Opt. Mater. 117 (Jul) (2021) 111182.

33. **Abduvayitov A. A., Tashmukhamedova D. A., Umirzakov B. E., et al.,** Effect of argon ion bombardment on the composition, electronic structure and physical properties of cadmium fluoride, St. Petersburg State Polytechnical University Journal. Physics and Mathematics. 17 (3) (2024) 87–96.

34. **Tashmukhamedova D. A.,** Study of composition and electronic structure of $CoSi_2$/Si interface, Bull. Russ. Acad. Sci., Phys. 70 (8) (2006) 1409–1411.

35. **Mahmood W., Awan S.U., Din A.U., et al.,** Pronounced impact of *p*-type carriers and reduction of bandgap in semiconducting ZnTe thin films by Cu doping for intermediate buffer layer in heterojunction solar cells, Materials. 12 (8) (2019) 1359.

36. **Donaev S. B., Tashatov A. K., Umirzakov B. E.,** Effect of Ar+-ion bombardment on the composition and structure of the surface of $CoSi_2$/Si(111) nanofilms, J. Surf. Invest.: X-Ray, Synchrotron Neutron Tech. 9 (2) (2015) 406–409.

37. **Abduvayitov A. A., Boltaev Kh. Kh., Rozikov G. A.,** Study of the composition of uncontrolled impurities and the profiles of their distribution at the Ni–CdS interface, J. Surf. Invest.: X-Ray, Synchrotron Neutron Tech. 16 (5) (2022) 860–863.

38. **Ghosh K., Ghorai G., Sahoo P. K.,** Cathodoluminescence and structural properties of ZnTe nanocrystals synthesized from Te/ZnO thin films, J. Alloys Compnd. 960 (15 Oct) (2023) 170655.

39. **Davis L. E., MacDonald N.C., Palmberg P.W., et al.,** Handbook of Auger electron spectroscopy, 2-nd ed., Physical Electronics Industry Inc., Minnesota (USA), 1976.

40. **Boltaev Kh. Kh., Tashmukhamedova D. A., Umirzakov B. E.,** Structure and electronic properties of nanoscale phases and nanofilms of metal silicides produced by ion implantation in combination with annealing, J. Surf. Invest.: X-ray, Synchrotron Neutron Tech. 8 (2) (2014) 326–331.

СПИСОК ЛИТЕРАТУРЫ

1. **Iniewski K.** CdTe and CdZnTe materials: Material properties and applications. Cham, Switzerland: Springer, 2024. 259 p.

2. **Suthar D., Chuhadiya S., Sharma R., Himanshu, Dhaka M. S.** An overview on the role of ZnTe as an efficient interface in CdTe thin film solar cells: A review // Materials Advances. 2022. Vol. 3. No. 22. Pp. 8081–8107.

3. **Zhao Y., Jia Z., Lin Q.** Optoelectronic properties and charge carrier dynamics of polycrystalline ZnTe thin films // The Journal of Physical Chemistry Letters. 2025. Vol. 16. No. 24. Pp. 5979–5985.

4. **Yılmaz S., Başol B. M., Olğar M. A., Bayazıt T., Küzükömeroğlu T., Bacaksız E.** Comparative analysis of chloride-treated ZnTe films in photodetector devices // Materials Science in Semiconductor Processing, 2025. Vol. 198. 1 November. P. 109733.

5. **Zhang L., Liu C., Yang Q., Cui L., Zeng Y.** Growth and characterization of highly nitrogen doped ZnTe films on GaAs (001) by molecular beam epitaxy // Materials Science in Semiconductor Processing. 2015. Vol. 29. January. Pp. 351–356.

6. **Эргашов Е. С., Ташмухамедова Д. А., Джурабекова Ф. Г., Умирзаков Б. Е.** Влияние микронеоднородностей поверхности на состав и электронные свойства пленок CdTe/Mo(111) // Известия Российской академии наук. Серия физическая. 2016. Т. 80. № 2. Ст. 157.

7. **Bagaev V. S., Zaytsev V. V., Kalinin V. V., Oktyabrskii S. R., Plotnikov A. F.** Excitonic luminescence of CdTe and $Cd_{0.87}Zn_{0.13}Te$ submonolayers in ZnTe films grown by molecular beam epitaxy // Solid State Communications. 1993. Vol. 88. No. 10. Pp. 777–780.

8. **Karczewski G., Maćkowski S., Kutrowski M., Wojtowicz T., Kossut J.** Photoluminescence study of CdTe/ZnTe self-assembled quantum dots // Applied Physics Letters. 1999. Vol. 74. No. 20. Pp. 3011–3013.

9. **Moger S. N., Mahesha M. G.** Investigation on ZnTe/$Cd_xZn_{1-x}Te$ heterostructure for photodetector applications // Sensors and Actuators A: Physical. 2020. Vol. 315. 1 November. P. 112294.

10. **Hernández C. V.** Introduction to Raman spectroscopy and its applications. Cham, Switzerland: Springer, 2025. 244 p.

11. **Kapitonov A. M., Woggon U., Kayser D., Hommel D., Itoh T.** Luminescence of epitaxial sub-monolayer CdSe nanostructures in ZnSe // Journal of Luminescence. 2005. Vol. 112. No. 1–4. Pp. 177–180.

12. **Kim J. S., Kim H. M., Park H. L., Choi J. C.** Growth and optical characterization of single quantum well structure of submonolayer ZnS/ZnTe // Solid State Communications. 2006. Vol. 137. No. 3. Pp. 115–119.

13. **Umirzakov B. E., Tashmukhamedova D. A., Boltaev E. U., Dzhurakhalov A. A. O**btaining of epitaxial films of metal silicides by ion implantation and molecular beam epitaxy // Materials Science and Engineering: B –Solid State Materials for Advanced Technology. 2003. Vol. 101. No. 1–3. Pp. 124–127.

14**. Kryshtab T., Andraca J. A., Borkovska L. V., Korsunska N. O., Venger Ye. F., Sadofyev Yu. G**. Effect of CdTe monolayer insertion on CdZnTe/ZnTe quantum well characteristics // Microelectronics Journal. 2008. Vol. 39. No. 3–4. Pp. 418–422.

15. **Fan J., Ouyang L., Liu X., Ding D., Furdyna J. K., Smith D. J., Zhang Y. H.** Growth and material properties of ZnTe on GaAs, InP, InAs and GaSb (001) substrates for electronic and optoelectronic device applications // Journal of Crystal Growth. 2011. Vol. 323. No. 1. Pp. 127–131.

16. **Умирзаков Б. Е., Донаев С. Б.** Создание ионной бомбардировкой упорядоченных зародышей для получения наноразмерных структур Si на поверхности пленок CaF_2 // Поверхность. Рентгеновские, синхротронные и нейтронные исследования. 2017. № 7. С. 70–73.

17. **Agekyan V., Chukeev M., Karczewski G., Serov A., Filosofov N., Reznitski A.** Exciton spectra and energy transfer in CdTe/ZnTe double quantum wells grown by atomic-layer epitaxy // Semiconductors. 2019. Vol. 53. No. 16. Pp. 2060–2063.

18. **Абдуваитов А. А., Болтаев Х. Х., Умирзаков Б. Е., Ташмухамедова Д. А., Абдурахманов Г.** Изучение изменения состава поверхности CdTe при имплантации ионов O^{2+} и последующего отжига // Известия Российской академии наук. Серия физическая. 2024. Т. 88. № 11. С. 1830–1834.

19. **Sawicki K., Malinowski F. K., Galkowski K., Jakubczyk T., Kossacki P., Pacuski W., Suffczinski J.** Single-color, *in situ* photolithography marking of individual CdTe/ZnTe quantum dots containing a single Mn^{2+} ion // Applied Physics Letters. 2015. Vol. 106. No. 1. P. 012101.

20. **Samin A. J., Petrosky J. C.** An analysis of point defects in ZnTe using density functional theory calculations // Journal of Alloys and Compounds. 2022. Vol. 921. 15 November. P. 166017.

21. **Рыжков М. С., Козлов Д. А., Худайбердиев Д. А., Квон З. Д., Михайлов Н. Н.** Интерференционный транспорт в двумерном топологическом изоляторе в CdHgTe квантовой яме // Письма в ЖЭТФ. 2023. Т. 117. № 1–2 (1). С. 50–54.

22. **Щербаков И. П., Дунаев А. А., Еронько С. Б., Чмель А. Е.** Спектроскопическое исследование примесных и собственных нарушений строения кристаллитов в керамике ZnTe при механической обработке // Письма в ЖТФ. Т. 47. № 4. С. 26–28.

23. **Тарасов А. С., Михайлов Н. Н., Дворецкий С. А., Менщиков Р. В., Ужаков И. Н., Кожухов А. С., Федосенко Е. В., Терещенко О. Е.** Получение атомарно-чистых и структурно-упорядоченных поверхностей эпитаксиальных пленок CdTe для последующей эпитаксии // Физика и техника полупроводников. 2021. Т. 55. № 9. С. 748–753.

24. **Martinez A. M., Giudici P., Trigubo A. B., D'Elia R., Heredia E., Ramelli R., Gonzalez R., Aza F., Gilabert U.** Crystalline quality, composition homogeneity, tellurium precipitates/inclusions concentration, optical transmission, and energy band gap of Bridgman grown single-crystalline $Cd_{1-x}Zn_xTe$ ($0 \le x \le 0.1$) // Materials. 2021. Vol. 14. No. 15. P. 4207.

25. **Дворецкий С. А., Ступак М Ф., Михайлов Н. Н., Макаров С. Н., Елесин А. Г., Верхогляд А. Г.** Исследование кристаллического состояния слоев молекулярно-лучевой эпитаксии гетероструктур (013)HgCdTe/CdTe/ZnTe/GaAs методом генерации второй гармоники // Физика и техника полупроводников. 2022. Т. 8 № .56. С. 787–780.

26. **Ступак М Ф., Михайлов Н. Н., Дворецкий С. А., Якушев М. В., Икусов Д. Г., Макаров С. Н., Елесин А. Г., Верхогляд А. Г.** Возможности характеризации кристаллических параметров структур $Cd_xHg_{1-x}Te$ на подложке из GaAs методом генерации на отражение второй гармоники зондирующего излучения // Физика твердого тала. 2020. Т. 62. № 2. С. 252–259.

27. **Ушаков В. В., Клевков Ю. В.** Микрофотолюминесценция нелегированного монокристаллического теллурида цинка, полученного неравновесными парофазными методами // Физика и техника полупроводников. 2005. Т. 39. № 9. С. 1029–1033.

28. **Ступак М Ф., Дворецкий С. А., Михайлов Н. Н., Макаров С. Н., Елесин А. Г.** Измерение локальных напряжений в поверхностных слоях многослойных структур нуль-методом с использованием фазового синхронизма // Письма в Журнал технической физики. 2024. Т. 50. № 1. С. 32–35.

29. **Chemam R., Bouabellou A., Grob J. J., Muller D., Schmerber G.** ZnTe nanoparticles formed by ion implantation in a SiO_2 layer on silicon // Nuclear Instruments and Methods in Physics Research B: Beam Interactions with Materials and Atoms. 2004. Vol. 216. February. Pp. 116–120.

30. **Umirzakov B. E., Tashmukhamedova D. A., Ruzibaeva M. K., Djurabekova F. G., Danaev S. B.** Investigation of change of the composition and structure of the CaF_2/Si films surface at the low-energy bombardment // Nuclear Instruments and Methods in Physics Research B: Beam Interactions with Materials and Atoms. 2014. Vol. 326. 1 May. Pp. 322–325.

31. **Исаханов З. А., Мухтаров З. Э., Умирзаков Б. Е., Рузибаева М. К.** Оптимальные режимы ионной имплантации и отжига для стимулирования вторичной отрицательной ионной эмиссии // Журнал технической физики. 2011. Т. 8. № 4. С. 117–120.

32. **Hassan A. M., Diab F., Kotp E. F., Al-Kashef G., Shaaban E. R., Metawa A. E.** Implantation of Cu onto ZnTe thin film using plasma focus device for optoelectronic applications // Optical Materials. 2021. Vol. 117. July. P. 111182.

33. **Abduvayitov A. A., Tashmukhamedova D. A., Umirzakov B. E., Khujaniyozov J. B., Bekpulatov I. R., Loboda V. V.** Effect of argon ion bombardment on the composition, electronic structure and physical properties of cadmium fluoride // St. Petersburg State Polytechnical University Journal. Physics and Mathematics. 2024. Vol. 17. No. 3. Pp. 87–96.

34. **Ташмухамедова Д. А.** Исследование состава и электронной структуры границы раздела $CoSi_2$/Si // Известия Российской академии наук. Серия физическая. 2006. Т. 70. № 8. С. 1228–1230.

35. **Mahmood W., Awan S.U., Din A.U., et al.** Pronounced impact of *p*-type carriers and reduction of bandgap in semiconducting ZnTe thin films by Cu doping for intermediate buffer layer in hetero-junction solar cells // Materials. 2019. Vol. 12. No. 8. P. 1359.

36. **Донаев С. Б., Ташатов А. К., Умирзаков Б. Е.** Влияние бомбардировки ионами Ar^+ на состав и структуру поверхности нанопленок $CoSi_2$/Si(111) // Поверхность. Рентгеновские, синхротронные и нейтронные исследования. 2015. № 4. С. 95–98.

37. **Абдувайитов А. А., Болтаев Х. Х., Розиков Г. А.** Изучение состава неконтролируемых примесей и профиля их распределения на границе раздела Ni–CdS // Поверхность. Рентгеновские, синхротронные и нейтронные исследования. 2022. № 10. С. 48–51.

38. **Ghosh K., Ghorai G., Sahoo P. K.** Cathodoluminescence and structural properties of ZnTe nanocrystals synthesized from Te/ZnO thin films // Journal of Alloys and Compounds. 2023. Vol. 960. 15 October. P. 170655.

39. **Davis L. E., MacDonald N.C., Palmberg P.W., Riach G.E., Weber R.E.** Handbook of Auger electron spectroscopy. Second edition. Minnesota (USA): Physical Electronics Industry Inc., 1976. 252 p.

40. **Болтаев Х. Х., Ташмухамедова Д. А., Умирзаков Б. Е.** Состав и электронные свойства наноразмерных фаз и нанопленок силицидов металлов, созданных методом ионной имплантации в сочетании с отжигом // Поверхность. Рентгеновские, синхротронные и нейтронные исследования. 2014. № 4. С. 24–29.

THE AUTHORS

KHUJANIYOZOV Jumanazar B.
Tashkent State Technical University Named after Islam Karimov
2 Universitet St., Almazar, Tashkent, 100095, Republic of Uzbekistan
KhujaniyozovJB@mail.ru
ORCID: 0000-0001-6067-8196

UMIRZAKOV Baltokhodja E.
Tashkent State Technical University Named after Islam Karimov
2 Universitet St., Almazar, Tashkent, 100095, Republic of Uzbekistan
be.umirzakov@gmail.com
ORCID: 0000-0002-9815-2111

TASHMUKHAMEDOVA Dilnoza A.
Tashkent State Technical University Named after Islam Karimov
2 Universitet St., Almazar, Tashkent, 100095, Republic of Uzbekistan
ftmet@mail.ru
ORCID: 0000-0001-5813-7518

LOBODA Vera V.
Peter the Great St. Petersburg Polytechnic University
29 Politechnicheskaya St., St. Petersburg, 195251, Russia
vera_loboda@mail.ru
ORCID: 0000-0003-3103-7060

ABDUVAYITOV Akbarjon A.
Tashkent State Technical University Named after Islam Karimov
2 Universitet St., Almazar, Tashkent, 100095, Republic of Uzbekistan
akbarjon.abduvayitov@gmail.com
ORCID: 0000-0002-5732-6103

СВЕДЕНИЯ ОБ АВТОРАХ

ХУЖАНИЁЗОВ Жуманазар Бобокулович – *кандидат физико-математических наук, доцент кафедры общей физики Ташкентского государственного технического университета имени Ислама Каримова.*
2100095, *Республика* Узбекистан, г. Ташкент, Университетская ул., 2
KhujaniyozovJB@mail.ru
ORCID: 0000-0001-6067-8196

УМИРЗАКОВ Балтоходжа Ерматович – *доктор физико-математических наук, профессор кафедры общей физики Ташкентского государственного технического университета имени Ислама Каримова.*
2100095, Республика Узбекистан, г. Ташкент, Университетская ул., 2
be.umirzakov@gmail.com
ORCID: 0000-0002-9815-2111

ТАШМУХАМЕДОВА Дилноза Артикбаевна – *доктор физико-математических наук, профессор кафедры технологий производства электронных аппаратов Ташкентского государственного технического университета имени Ислама Каримова.*
2100095, Республика Узбекистан, г. Ташкент, Университетская ул., 2
ftmet@mail.ru
ORCID: 0000-0001-5813-7518

ЛОБОДА Вера Владимировна – *кандидат физико-математических наук, директор Высшей школы электроники и микросистемной техники Санкт-Петербургского политехнического университета Петра Великого.*
195251, Россия, г. Санкт-Петербург, Политехническая ул., 29
vera_loboda@mail.ru
ORCID: 0000-0003-3103-7060

АБДУВАЙИТОВ Акбаржон Абдумаджитович – *доктор физико-математических наук, профессор кафедры общей физики Ташкентского государственного технического университета имени Ислама Каримова.*
2100095, Республика Узбекистан, г. Ташкент, Университетская ул., 2
akbarjon.abduvayitov@gmail.com
ORCID: 0000-0002-5732-6103

Received 14.01.2026. Approved after reviewing 12.02.2026. Accepted 13.02.2026.
Статья поступила в редакцию 14.01.2026. Одобрена после рецензирования 12.02.2026. Принята 13.02.2026.

© Peter the Great St. Petersburg Polytechnic University, 2026